A primary model of decoherence in neuronal microtubules based on the interaction Hamiltonian between microtubules and plasmon in the neurons

Zuoxian Xiang(向左鲜), Chuanxiang Tang(唐传祥)†, and Lixin Yan(颜立新)

Department of Engineering Physics, Tsinghua University, Beijing 100084, *China*

(Received 19 November 2018; revised manuscript received 3 December 2018; published online 5 March 2019)

Microtubules (MTs) are part of the cellular cytoskeleton; they play roles in activities such as cell division and maintenance of cell shape. In recent years, MTs have been thought to be involved in the storing and processing information; several models have been developed to describe the information-processing ability of MTs. In these models, MTs are considered as a device that can transmit quantum information. However, MTs are affected by the "wet and warm" cellular environment, thus, calculating the decoherence time becomes essential. Many researchers have attempted to calculate this parameter, but the values obtained vary markedly. Previous studies considered the cellular environment as a distant ion; this treatment is somewhat simplified. In this study, we develop a model to determine the decoherence time in neuronal MTs while considering the interaction effects of the neuronal fluid environment. The neuronal environment is considered as a plasmon reservoir. The coupling between MTs and neuronal environment occurs due to the interaction between dipoles and plasmon. The interaction Hamiltonian is derived by using the second quantization method, and the coupling coefficient is calculated. Finally, the decoherence time scale is estimated according to the interaction Hamiltonian. In this paper, the time scale of decoherence in MTs is approximately 1 fs-100 fs. This model may be used as a reference in other decoherence processes in biological tissues.

Keywords: consciousness, microtubules, quantum decoherence

PACS: 87.10.–e, 87.10.Vg

DOI: 10.1088/1674-1056/28/4/048701

CPB Online In-Press

1. Introduction

Quantum theory is one of the greatest discoveries of the twentieth century. In recent years, quantum effects in biological systems have been discovered in several areas, including olfaction,[1,2] avian magnetoreception,[3,4] photosynthesis,[5–9] quantum entanglement in living bacteria,[10] and so on.[11] Theoretical study of quantum effect in bio-systems and its possible relevance to explaining the functional properties of these systems are also drawing rapid attention, such as consciousness in the brain.

How to explain consciousness? Classical or quantum? It is so mysterious and researchers have proposed many models.[12–24] Some studies suggested that the quantum effect might play an important role in the functioning of the brain.[16–24] Penrose and Hameroff proposed the orchestrated objective reduction (Orch OR) model, which suggests that microtubules (MTs) in neurons act as a quantum computer,[18–20,24] Fisher proposed that quantum entanglement may exist between two neurons.[23]

Decoherence is an important phenomenon in quantum information. The "warm, wet, and noisy" environment might destroy the quantum state,[26–29] thus the decoherence time scale τ is an important parameter to the quantum model.

To study the decoherence process in MTs, researchers determined this parameter according to different mechanisms of decoherence, including quantum gravity,[18] cavity quantum electrodynamics (QED) model,[25,26] and single ion-MT interactions; these results are listed in Table 1 and the value of decoherence time varies greatly.

Table 1. Decoherence time scales and their mechanisms.

Mechanisms	Researchers	Timescale
Quantum gravity	Penrose	~ 10 ms
Cavity QED	Mavromatos	0.1 ns$\sim$0.1 ms
Ion-dipole	Tegmark	~ 0.1 ps
Ion-dipole	Hagan *et al.*	1 μs–10 μs

Decoherence mainly derives from the interaction between quantum systems and the environment. There are 4 basic interactions that have been discovered in nature; in the range of molecule interactions, the main interaction between environment and tubulin dimers is electromagnetic interaction. In this paper, a model based on the electromagnetic interaction Hamiltonian between microtubules and plasmon in the neurons is proposed. Previous studies considered the effect of a single ion on the decoherence process in MTs; however, cells are known to contain different kinds of ions that have different charges and masses, *i.e.*, some ions have positive charge, whereas others have negative charge. Over a long time scale, cells can be considered to be electrically neutral; however, this is not true over very short time scales. Therefore, the decoherence rates cannot be calculated only considering the effect of a single ion since decoherence is a result of the interaction

†Corresponding author. E-mail: tang.xuh@tsinghua.edu.cn

© 2019 Chinese Physical Society and IOP Publishing Ltd

between tubulin dimers and cellular fluid environment. In this paper, the interaction Hamiltonian is constructed by using the second quantization method, and the decoherence time is estimated according to the interaction Hamiltonian.

This article is organized as follows. Section 2 includes the introduction for decoherence mechanisms in our model, as well as the total Hamiltonian of tubulin dimers and cell fluid environment; the decoherence timescale τ are computed and how τ changes with environment parameters will be discussed. In Section 3, other mechanisms of decoherence will be discussed, and some important formulas and their derivations are given in the appendix.

2. Decoherence rates

In this section, the decohenrence mechanisms in MTs will be discussed. MT is a hollow cylinder with an outer diameter of 24 nm and an inner diameter of 15 nm. The basic unit of MT is tubulin dimer which has two subunits (denoted by α and β); all of the tubulin dimers form MT crystal lattice by helical encircle. The tubulin dimers have different kinds of conformational states which are regarded as quantum bit in Orch model, and MTs can store information owing to different combinations of these conformational states. Electron transition in each tubulin dimer could change the conformational states, and the MT is a polar molecule and has intrinsic electric dipole moment (Fig. 1).[25]

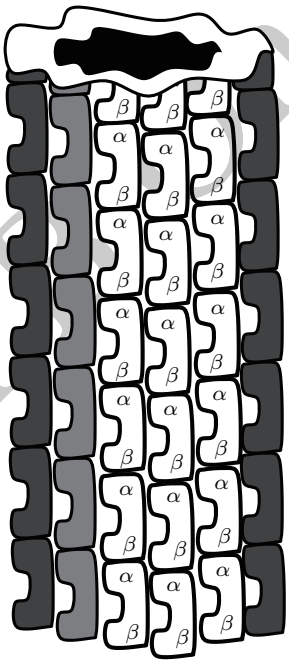


Fig. 1. The structure diagram of MTs.

2.1. Mechanisms of decoherence

The cellular fluid is considered to have both positive and negative charges (similar to plasma), and thus two basic and very important parameters are used to describe the it, namely Debye length λ_D and plasma frequency ω_p; these two parameters will be discussed compendiously and their range will be given.

The Debye length λ_D represents the space scale when the plasma is kept as a neutral state and is determined by

$$\lambda_D = 1/\sqrt{\sum_k \frac{n_{k,0}q_k^2}{\varepsilon k_B T}}, \tag{1}$$

where $n_{k,0}$ is the average density of the k-th kind of ion, q_k is the quantity of charge, $\varepsilon = 80\varepsilon_0$ is the dielectric constant of water, k_B is the Boltzmann constant, and T is the temperature of the cellular fluid. For physiological Ringer solution, $\lambda_D \sim 0.7$ nm,[29] and in the following calculation, the value of λ_D is set to be around 0.7 nm.

The surface of tubulin dimers have net charge,[30] so a counterion layer will be formed because of the Debye shielding. The thickness of the counterions is approximately λ_D, as shown in Fig. 2. The counterions could shield the interaction between MTs and the environment, as shown in Appendix C, the coupling coefficient is decreased if the shielding effect is considered.

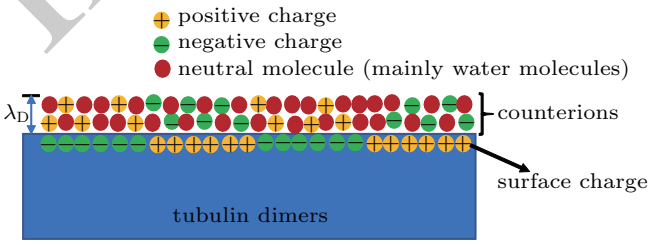


Fig. 2. Schematic diagram of counterion layer with a thickness of λ_D.

The second parameter is called plasma frequency, which describes the collective oscillations of ions and is determined by

$$\omega_p = \sqrt{\sum_k \frac{n_{k,0}q_k^2}{\varepsilon m_k}}. \tag{2}$$

For typical parameters in a cell,[29] $[K^+]_{in} = 400$ mmol/L, $[Na^+]_{in} = 50$ mmol/L$[Cl^-]_{in} = 52$ mmol/L, $\omega_p \approx 0.6$ THz. Therefore, in the following calculation, the value of ω_p is set to be around 0.6 THz.

When the plasmon is in an excited state, the electric neutrality is destroyed, and some net charges appear. The net charges can interact with the dipole in the tubulin dimmers, as shown in Fig. 3. As shown in Appendix A, the local ion density fluctuation could excite ion density waves. There are different ion density waves, but the only one called plasma oscillation could be coupled with MTs, and the dispersion relation of plasma oscillation is

$$\omega^2(\boldsymbol{k}) = \omega_p^2 + \beta^2 k^2, \tag{3}$$

where β is the average value of ion thermal velocity, which has the same order of magnitude as the thermal velocity.

CPL Online In Press

The total Hamiltonian of the MT-environmental systems can be derived as follows:

$$\hat{H} = \hat{H}_{\mathrm{MT}} + \hat{H}_{\mathrm{e}} + \hat{H}', \tag{4}$$

where $\hat{H}_{\mathrm{MT}}$ is the Hamiltonian of the excited systems in the MTs, $\hat{H}_{\mathrm{e}}$ is the Hamiltonian of the plasmons in the cellular fluid environment, and $\hat{H}'$ represents the interaction between the MTs and cellular aqueous environment caused by the interactions between the dipole and net charges. $\hat{H}'$ is the reason for decoherence; if $\hat{H}' = 0$, the decoherence time is $\tau = \infty$.

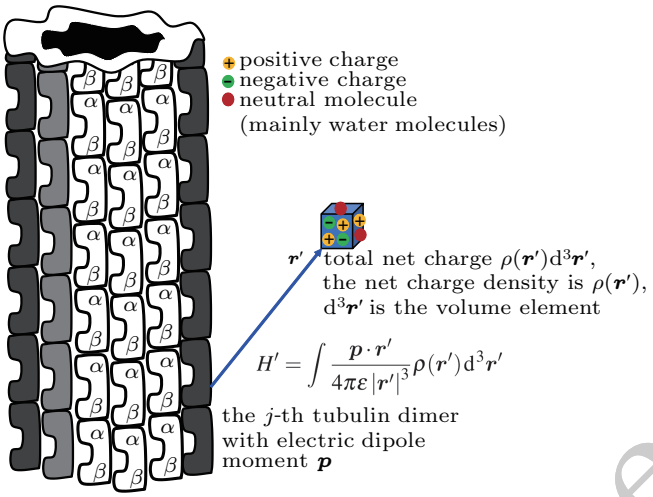


Fig. 3. Schematic diagram of the coupling between tubulin dimers and the cellular fluid environment.

As shown in Fig. 3, the interaction Hamiltonian between a single tubulin dimer with the electric dipole moment $\boldsymbol{p}$ and the cellular fluid environment can be shown as follows:

$$H' = \int \frac{\boldsymbol{p}\cdot\boldsymbol{r}'}{4\pi\varepsilon|\boldsymbol{r}'|^3}\rho(\boldsymbol{r}')\mathrm{d}^3\boldsymbol{r}'. \tag{5}$$

2.2. Computation method of decoherence timescale

Now, the total Hamiltonian equation (4) will be derived; some basic assumption or approximation is listed below, and will be discussed in Section 3 and appendix.

(i) Water is treated as an medium with a dielectric constant $\varepsilon = 80\varepsilon_0$, and detailed interaction of ion-water molecules and MT-water molecules is ignored.

(ii) Due to the Debye shielding, plasma oscillations could only be excited above the Debye length, that is to say, the wave number$k$has an upper limit of $k = k_{\mathrm{D}} = 2\pi/\lambda_{\mathrm{D}}$; in our calculation, we consider k will decay rapidly as a small quantity for the short wavelength modes.

(iii) Random phase approximation (RPA) for many-particles system, In equilibrium state or near equilibrium state, as the position of particles is random, $\sum_i \exp(\mathrm{i}\boldsymbol{k}\cdot\boldsymbol{r}_i) = 0$ unless $k = 0$.

(iv) The tubulin dimers are seen as a mass point with electric dipole moment $\boldsymbol{p}$.

As introduced in Subsection 2.1, the tubulin dimers have different conformational states, denoted by $|k\rangle$, and let $\hat{c}_k^\dagger, \hat{c}_k$ be the creation operator and annihilation operator of the quantum state $|k\rangle$, so the Hamiltonian of tubulin dimers can be expressed by

$$\hat{H} = \sum_n \hbar\Omega_n \hat{c}_n^\dagger \hat{c}_n, \tag{6}$$

where $\hbar\Omega_n$ is the eigenvalue of quantum state $|n\rangle$; the numerical estimation of $\hbar\Omega_n$ can be seen in Ref. [21].

The detailed calculation of $\hat{H}_{\mathrm{e}}$, $\hat{H}'$ will be given in Appendix A and Appendix B, and the total Hamiltonian of the MTs and cellular environment can be expressed as follows:

$$\begin{aligned}\hat{H} = &\sum_n \hbar\Omega_n \hat{c}_n^\dagger \hat{c}_n \\ &+ \sum_{\boldsymbol{k}} \hbar\omega(\boldsymbol{k}) \left[\hat{b}^\dagger(\boldsymbol{k})\hat{b}(\boldsymbol{k}) + \frac{1}{2}\right] \\ &+ \sum_{n,\boldsymbol{k}} \mu_{n,\boldsymbol{k}} \hat{c}_n^\dagger \hat{c}_n \left[\hat{b}^\dagger(\boldsymbol{k}) + \hat{b}(\boldsymbol{k})\right],\end{aligned} \tag{7}$$

where $\omega(\boldsymbol{k}) = \sqrt{\omega_{\mathrm{p}}^2 + \beta^2 k^2}$ is the dispersion relation of plasma oscillation, $\hat{b}^\dagger(\boldsymbol{k})$ and $\hat{b}(\boldsymbol{k})$ are the creation operator and annihilation operator of plasma oscillations, respectively, and the coupling coefficient $\mu_{n,\boldsymbol{k}}$ is given by

$$\mu_{n,\boldsymbol{k}} = \mathrm{i}\lambda_{n,\boldsymbol{k}} = \frac{\boldsymbol{p}_n\cdot\boldsymbol{k}}{2k}\sqrt{\frac{\hbar\omega(\boldsymbol{k})}{2\varepsilon}}\frac{\sin(k\lambda_{\mathrm{D}})}{(k\lambda_{\mathrm{D}})}. \tag{8}$$

Equation (8) is given in Appendix C, and $\boldsymbol{p}_n$ is the electric dipole moment in state $|n\rangle$.

Next, Tolkunov's model is used,[31,32] which describes the interaction between the spin system and Boson thermal reservoir. In 2-level approximation, the Hamiltonian equation (7) of our model is the same with that of Tolkunov's in form, so the non-diagonal elements of density matrix will also change with time in the same way

$$q_n(t) = q_n(0)\exp\left\{-\sum_{\boldsymbol{k}} \frac{8|\lambda_{n,\boldsymbol{k}}|^2 \sin^2\dfrac{\omega(\boldsymbol{k})t}{2}}{\hbar^2\omega^2(\boldsymbol{k})\tanh\dfrac{\hbar\omega(\boldsymbol{k})}{2k_{\mathrm{B}}T}}\right\}. \tag{9}$$

Here, $\sum_{\boldsymbol{k}} = \frac{1}{(2\pi)^3}\int \mathrm{d}^3\boldsymbol{k}$, and the integral region is $0 < k < 2\pi/\lambda_{\mathrm{D}}$. The plasma-like oscillations will be excited only when the wavelength is larger than the Debye length.[33] Therefore, it could only be used to refer to the excited state, and equation (9) will become

$$q_n(t) = q_n(0)\exp\left[-G(t)\right], \tag{10}$$

where

$$G(t) = \frac{p_n^2}{6\varepsilon\hbar\pi^2\lambda_{\mathrm{D}}^2}\int_0^{2\pi/\lambda_{\mathrm{D}}} \frac{\sin^2(k\lambda_{\mathrm{D}})\sin^2\dfrac{\omega(\boldsymbol{k})t}{2}}{\omega(\boldsymbol{k})\tanh\dfrac{\hbar\omega(\boldsymbol{k})}{2k_{\mathrm{B}}T}}\mathrm{d}k. \tag{11}$$

Obviously, $G(t) > 0$. In the quantum information theory, the decoherence process is reflected in the damping of the

CPB Online In-Press

nondiagonal element of the density matrix, so we define decoherence time τ as the timescale when $q_n(t)$ decays into $q_n(0)/e$, namely

$$G(\tau) = 1. \tag{12}$$

Equations (11) and (12) could be used to compute decoherence time.

2.3. Typical order of magnitude of decoherence timescale

In this section, the typical value of decoherence time scale will be estimated by Eqs. (11) and (12). The parameters in Eq. (10) are chosen as follows:

$p_n = 3 \times 10^{-28}$ C·m is the electric dipole moment of tubulin dimer.[25]

$\varepsilon = 80\varepsilon_0$ is the dielectric constant of water.[29]

$\lambda_D \sim 0.7$ nm, $\omega_p = 0.6$ THz; these two basic plasma parameters have been discussed in Subsection 2.1.

$T = 310$ K is the environment temperature.

$\beta = 300$ m/s since it has the same order of magnitude with the thermal velocity.

$k_B = 1.38 \times 10^{-23}$ J/K is the Boltzmann's constant.

$\hbar = 1.0546 \times 10^{-34}$ J·s is the Planck's constant.

The function $G(t)$ can be computed in a numerical method (Fig. 4). Set $G(\tau) = 1$ and the decoherence time could be easily obtained

$$\tau = 16.2 \text{ fs}. \tag{13}$$

The decoherence timescale is about 10 fs.

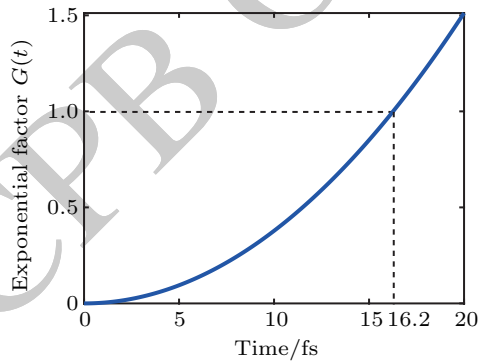


Fig. 4. Schematic diagram of how to compute the decoherence time by the exponential factor $G(t)$.

2.4. The dependence of decoherence time with other parameters

Decoherence time may change with other parameters; how these parameters affect the decoherence time will be studied in this section. As discussed in Subsection 2.3, the typical time scale for decoherence is $T_0 = 10$ fs. So set $T_0 = 10$ fs as the time unit, six dimensionless physical quantities are shown below

$$\begin{cases} \tau_0 = \dfrac{t}{T_0}, & K = k\lambda_D, \\ \alpha_1 = \omega_p T_0, & \alpha_2 = \dfrac{\beta T_0}{\lambda_D}, \\ \alpha_3 = \dfrac{\hbar\omega_p}{2k_B T}, & \alpha_4 = \dfrac{p_n^2 T_0}{6\varepsilon\hbar\pi^2\lambda_D^3}. \end{cases} \tag{14}$$

Then equations (11) and (12) become

$$G(\tau_0) = \alpha_4 \int_0^{2\pi} \frac{\sin^2(K)\sin^2\left(\dfrac{\tau_0}{2}\sqrt{\alpha_1^2+\alpha_2^2K^2}\right)}{\sqrt{\alpha_1^2+\alpha_2^2K^2}\tanh\left(\dfrac{\alpha_3}{\alpha_1}\sqrt{\alpha_1^2+\alpha_2^2K^2}\right)}\,\mathrm{d}K, \tag{15a}$$

$$G(\tau/T_0) = 1. \tag{15b}$$

The typical values of these parameters are given in Subsection 2.3; in this section, their values are given in a wide range as follows:

$$\begin{aligned} &\omega_p = 0.06 \text{ THz} \sim 3.0 \text{ THz}, \\ &\beta = 60 \text{ m/s} \sim 1200 \text{ m/s}, \\ &\lambda_D = 0.21 \text{ nm} \sim 2.1 \text{ nm}, \\ &\varepsilon = 24\varepsilon_0 \sim 240\varepsilon_0, \\ &p_n = 0.09 \times 10^{-28} \text{ C·m} \sim 30 \times 10^{-28} \text{ C·m}, \\ &T = 90 \text{ K} \sim 900 \text{ K}. \end{aligned}$$

Here, some values may never be reached, such as $T = 900$ K, $\varepsilon = 240\varepsilon_0$, and so on; but the purpose in this model is to analyze how the decoherence time changes with physical parameter, so the parameter distribution is in a very wide range.

Case 1: Decoherence time changes with plasma frequency ω_p

As shown in Fig. 5, decoherence remains almost unchanged when the plasma frequency changes.

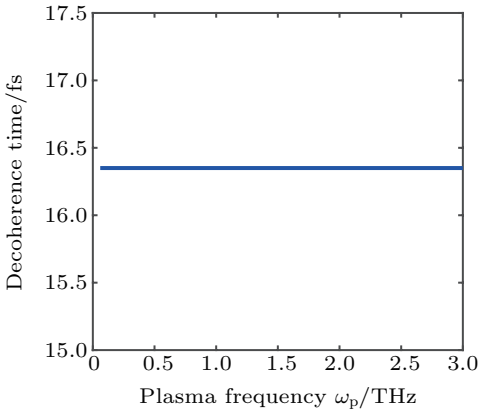


Fig. 5. Decoherence time changes with plasma frequency ω_p when other parameters are consistent with those in Subsection 2.3.

Case 2: Decoherence time changes with average thermal velocity β

As shown in Fig. 6, decoherence remains almost unchanged when the average thermal velocity β changes, similar to Case 1.

CPB Online In-Press

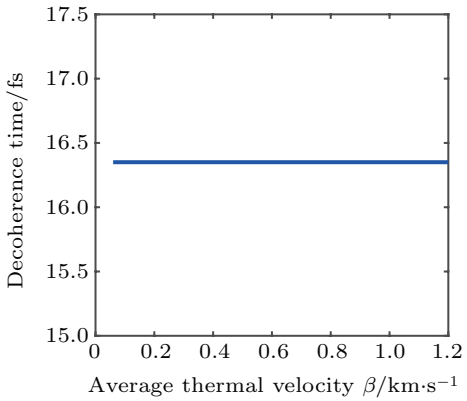


Fig. 6. Decoherence time changes with average thermal velocity β when other parameters are consistent with those in Subsection 2.3.

Case 3: Decoherence time changes with Debye length λ_D

In Fig. 7, the decoherence time increases with Debye length; since the plasma oscillation modes could only be excited when $k < 2\pi/\lambda_D$, a larger Debye length means that fewer modes will be excited, so the number of the modes interacting with MTs will decrease, and the decoherence time will increase.

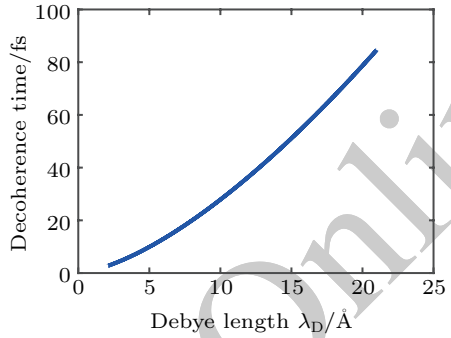


Fig. 7. Decoherence time changes with Debye length λ_D when other parameters are consistent with those in Subsection 2.3.

Use $\tau = C\lambda_D^s$ to fit the curve in Fig. 7 (or equivalently $\ln\tau = s\ln\lambda_D + \ln C$), the power exponent s and linearly dependent coefficient for $\ln\tau, \ln\lambda_D$ are

$$\begin{cases} s = 1.5003 \approx 1.5, \\ r = 0.99999993. \end{cases}$$

Doing the same work to other parameters and we find that $\tau = C\lambda_D^s$ could fit the relationship between τ, λ_D, so we can approximately consider that

$$\tau \approx C(\omega_p, \beta, T, p_n, \varepsilon)\lambda_D^{1.5}. \tag{16}$$

Case 4: Decoherence time changes with dielectric constant of water

In Fig. 8, the decoherence time increases with dielectric constant of water, and the reason is obvious. According to Eq. (5), a larger dielectric constant means the weaker interaction between MTs and environment.

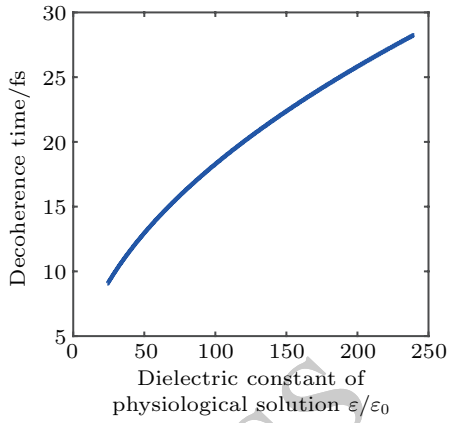


Fig. 8. Decoherence time changes with dielectric constant of water when other parameters are consistent with those in Subsection 2.3.

Doing the same work as Case 3 and we find that

$$\tau \approx C(\omega_p, \beta, T, p_n, \lambda_D)\varepsilon^{0.5}. \tag{17}$$

Case 5: Decoherence time changes with dipole moment of tubulin dimer p_n

In Fig. 9, we show the decoherence time decreases as the dipole moment of tubulin dimer increases; according to Eq. (5), the increase of the dipole moment will enhance the interaction between MTs and environment, and then the decoherence time will decrease.

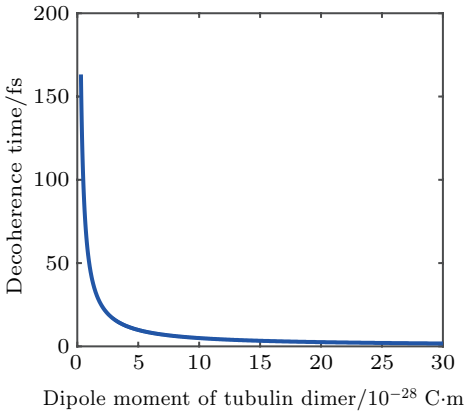


Fig. 9. Decoherence time changes with dipole moment of tubulin dimer p_n when other parameters are consistent with those in Subsection 2.3.

Doing the same work as Case 3 and we find that

$$\tau \approx C(\omega_p, \beta, T, \varepsilon, \lambda_D)p_n^{-1}. \tag{18}$$

Case 6: Decoherence time changes with environment temperature T

In Fig. 10, the decoherence time decreases as the environment temperature increases, and it is also easy to understand. The higher temperature means that more oscillation modes will be excited, and this will have a greater impact on the MTs, so the decoherence time decreases.

CPB Online In-Press

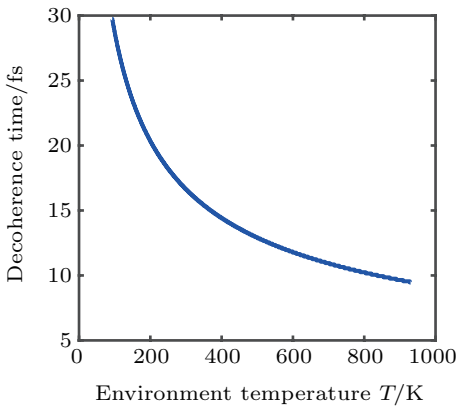


Fig. 10. Decoherence time changes with environment temperature T when other parameters are consistent with those in Subsection 2.3.

Doing the same work as Case 3 and we find that

$$\tau \approx C(\omega_{\rm p}, \beta, p_n, \varepsilon, \lambda_{\rm D}) T^{-0.5}. \tag{19}$$

According to Eqs. (16)–(19), the decoherence time could be approximately expressed as

$$\frac{\tau}{\tau(\omega_{\rm p}, \beta, p_{n0}, \varepsilon_0, \lambda_{\rm D0}, T_0)} \approx \left(\frac{\lambda_{\rm D}}{\lambda_{\rm D_0}}\right)^{1.5} \left(\frac{\varepsilon_r}{\varepsilon_{r0}}\right)^{0.5} \left(\frac{p_{n0}}{p_n}\right) \left(\frac{T_0}{T}\right)^{0.5}. \tag{20}$$

Since the decoherence time relies less on $\omega_{\rm p}$, β, then equation (20) will be changed into:

$$\frac{\tau}{\tau(p_{n0}, \varepsilon_0, \lambda_{\rm D0}, T_0)} \approx \left(\frac{\lambda_{\rm D}}{\lambda_{\rm D_0}}\right)^{1.5} \left(\frac{\varepsilon_r}{\varepsilon_{r0}}\right)^{0.5} \left(\frac{T_0}{T}\right)^{0.5} \frac{p_{n0}}{p_n}. \tag{21}$$

In fact, equation (21) could be proved, since the plasma frequency $\sqrt{\omega_{\rm p}^2 + \beta^2 k^2} \sim 1$ THz, the decoherence time $\tau \sim 10$ fs–100 fs, and the temperature $T \sim 100$ K. Therefore,

$$\begin{cases} \omega(\boldsymbol{k})\tau = \sqrt{\omega_{\rm p}^2 + \beta^2 k^2}\,\tau \ll 1, \\ \dfrac{\hbar\omega(\boldsymbol{k})}{2k_{\rm B}T} \ll 1. \end{cases} \tag{22}$$

Under the condition of Eq. (22), equation (12) could be approximately expressed as

$$G(t) = \frac{p_n^2}{6\varepsilon\hbar\pi^2\lambda_{\rm D}^2} \int_0^{2\pi/\lambda_{\rm D}} \frac{\sin^2(k\lambda_{\rm D}) \sin^2 \dfrac{\omega(\boldsymbol{k})t}{2}}{\omega(\boldsymbol{k}) \tanh \dfrac{\hbar\omega(\boldsymbol{k})}{2k_{\rm B}T}} {\rm d}k$$

$$\approx \frac{p_n^2 k_{\rm B} T t^2}{12\varepsilon\hbar^2\pi\lambda_{\rm D}^3}. \tag{23}$$

Then the decoherence time satisfies

$$\tau \approx \sqrt{\frac{12\varepsilon\hbar^2\pi\lambda_{\rm D}^3}{p_n^2 k_{\rm B} T}} \propto \varepsilon^{0.5} \lambda_{\rm D}^{1.5} p_n^{-1} T^{-0.5}. \tag{24}$$

Equation (24) could be used for calculating the decoherence time only under the condition of Eq. (22). However, equation (24) is useful for various actual parameters.

3. Conclusion and outlook

If the Orch OR model can be verified both in theory and experiment, the influence will be inestimable; however, the conformational state is affected by the "warm and wet" cellular environment, and the decoherence time is a very important parameter.

In this paper, the decoherence time scale is even smaller than 0.1 ps. This timescale is so short that quantum state will be destroyed by the cell solution environment soon. This model only considers the coupling between the tubulin dimers and ions in the cellular fluid system, treating the water as a medium and overlooking the interactions of MTs-water molecules; water molecules may shield some interactions of ion-MTs, and the interaction of water-ions and water-MTs may have influence on the decoherence process.[32,33] According to Eq. (24), if the interaction strength attenuates to ε $(0 < \varepsilon < 1)$, the decoherence will increase to $1/\sqrt{\varepsilon}$ than before; an enough decoherence requires $\varepsilon \ll 1$ and the strength of shielding by water molecules needs to be measured by experiment.

Other mechanism for decoherence that is not considered is the coherent pumping of the system via the environment.[21] According to Fröhlich's theory, if a system is strongly coupled to its environment via some degrees of freedom, and a coherent pumping source exists in environment, it might inhibit other degrees of freedom known as coherent oscillations.[35,36] Such oscillations might increase the decoherence time. Guanosine triphosphate (GTP) hydrolyzation in the cells might act as a pumping source. This mechanism was not considered in this paper.

Decoherence is an important phenomenon in quantum information. Decoherence mainly comes from the interaction of quantum systems with the environment. In the range of molecule interactions, the main interaction between environment and tubulin dimers is the electromagnetic interaction; the electromagnetic field comes from ions and thermal radiation of the environment. However, in this model, the thermal radiation is ignored, and in the range of room temperature, the thermal frequency spectrum mainly concentrates in the range of THz band. The water molecules in the cell environment could strongly absorb the THz photon and the model only takes into account the electromagnetic field from ions. Besides, if the thermal radiation is considered, the decoherence time would be smaller than the result given before, and it will not change the conclusion.

This model needs to be verified both experimentally and theoretically. This model may offer a helpful theoretical framework to compute the decoherence time in quantum biosystems, even though the environment of biological system is different. However, the electromagnetic interaction is essential in the scale of molecules, so this model could be used for reference when dealing with the interaction between the ions in cell

CPB Online In-Press

environment and dipoles of bio-molecules. The direct experiment to verify this model is hard to be carried out at this time, but with the development of ultrafast biophysics, quantum information, quantum optics, and imaging technology,[37–41] the experiment could be carried out in the future.

Appendix A: Dispersion relation of ion density wave

In Appendix A, the dispersion relation of ion density wave is derived by fluid theory. Note that n_i, m_i, $\boldsymbol{v}_i$, q_i represent the particle number density, ion mass, the macro velocity, and electric charge of the i-th ion. $\boldsymbol{E}$ is the space electric field, β_i is used to represent the ion thermal velocity, and $-m\beta_i^2\nabla n_i$ is the thermodynamic pressure of the i-th ion. Then according to fluid theory

$$\begin{cases} n_i m_i\left(\dfrac{\partial \boldsymbol{v}_i}{\partial t}+\boldsymbol{v}_i\cdot\nabla\boldsymbol{v}_i\right)=n_i q_i\boldsymbol{E}-m\beta_i^2\nabla n_i, \\ \dfrac{\partial n_i}{\partial t}+\nabla\cdot(n_i\boldsymbol{v}_i)=0, \\ \nabla\cdot\boldsymbol{E}=\dfrac{1}{\varepsilon}\sum\limits_i n_i q_i. \end{cases} \tag{A1}$$

In order to deduce intrinsic oscillation mode and its dispersion relation, linearization is done for Eq. (A1). For arbitrary physical quantity A, it is divided into two parts

$$A=\langle A\rangle+\tilde{A}, \tag{A2}$$

where $\langle A\rangle$ is the average value in equilibrium state, and $\tilde{A}$ is the fluctuate of A.

When $\tilde{A}\ll\langle A\rangle$ and $\langle\boldsymbol{v}_i\rangle=\langle\boldsymbol{E}\rangle=0$, equation (A1) changes to

$$\begin{cases} \langle n_l\rangle m_l\dfrac{\partial\tilde{v}_l}{\partial t}=\langle n_l\rangle q_l\tilde{E}-m\beta_l^2\nabla\tilde{n}_l, \\ \dfrac{\partial\tilde{n}_l}{\partial t}+\langle n_l\rangle\nabla\cdot\tilde{v}_l=0, \\ \nabla\cdot\tilde{E}=\dfrac{1}{\varepsilon}\sum\limits_l\tilde{n}_l q_l. \end{cases} \tag{A3}$$

Now, let us compute the eigenmode with intrinsic wavelength and frequency. Set $\tilde{A}=\tilde{A}_0\exp[\mathrm{i}(\boldsymbol{k}\cdot\boldsymbol{r}-\omega t)]$. Then the operator $\partial/\partial t=-\mathrm{i}\omega$, $\nabla=\mathrm{i}\boldsymbol{k}$, and equation (A3) changes to

$$\begin{cases} -\mathrm{i}\langle n_l\rangle\omega m_l\tilde{v}_l=\langle n_l\rangle q_l\tilde{E}-\mathrm{i}m\beta_l^2\tilde{n}_l\boldsymbol{k}, \\ -\mathrm{i}\tilde{n}_l\omega+i\langle n_l\rangle\boldsymbol{k}\cdot\tilde{v}_l=0, \\ \mathrm{i}\varepsilon\boldsymbol{k}\cdot\tilde{E}=\sum\limits_l\tilde{n}_l q_l. \end{cases} \tag{A4}$$

According to Eq. (A4), the eigen-equation is

$$\left(\omega^2-\frac{\langle n_l\rangle q_l^2}{\varepsilon m_l}-k^2\beta_l^2\right)\tilde{n}_l-\sum_{k\neq l}\frac{\langle n_l\rangle q_l q_k}{\varepsilon m_l}\tilde{n}_k=0. \tag{A5}$$

Or equivalent in matrix form

$$\Omega(\omega,k)\tilde{n}=0, \tag{A6}$$

where $\Omega_{l,k}=(\omega^2-k^2\beta_l^2)\delta_{kl}-\langle n_l\rangle q_l q_k/\varepsilon m_l$, and $\tilde{n}=(\tilde{n}_1,\tilde{n}_2,\ldots,\tilde{n}_M)^{\mathrm{T}}$. Set $f(\omega,k)=\det\Omega(\omega,k)$, equation (A6) must have untrivial solution to ensure eigenmode exits, so the dispersion relation is determined by

$$f(\omega,k)=0. \tag{A7}$$

Set $q_l=(-1)^{\upsilon_l}Z_l e$, where Z_l is the valence state of ions, *e.g.*, for Na^+ and Cl^-, $Z_l=1$, and for Ca^{2+}, $Z_l=2$, and υ_l represents the sign of ion charge, and

$$\upsilon_l=\begin{cases} 0 & \text{(for positive ion)}, \\ 1 & \text{(for negative ion)}. \end{cases} \tag{A8}$$

In long-wavelength limit $k\beta_l/\omega\ll1$, then

$$\begin{aligned} f(\omega,k)=&\left(\omega^2-\omega_{\mathrm{p}}^2-\beta^2k^2+o(k^2)\cdots\right) \\ &\times\prod_{j=1}^{M-1}\left[\omega^2-c_j^2k^2+o(k^2)\cdots\right], \end{aligned} \tag{A9}$$

where $\omega_l^2=\langle n_l\rangle q_l^2/\varepsilon m_l$, $\omega_{\mathrm{p}}^2=\sum\limits_{l=1}^{M}\omega_l^2$ is the plasma frequency, $\beta=\sqrt{\sum\limits_{l=1}^{M}\beta_l^2\omega_l^2/\omega_{\mathrm{p}}^2}$ is the average thermal velocity of all ions, and c_j $(j=2,3,\ldots,M)$ is the $M-1$ roots of the following equation

$$F(c)=\sum_j\frac{\omega_j^2}{c^2-\beta_j^2}=0, \tag{A10}$$

So M kinds of waves are obtained, and their dispersion relation is

$$\omega^2=\omega_{\mathrm{p}}^2+\beta^2k^2+o(k^2), \tag{A11a}$$

$$\omega^2=c_j^2k^2+o(k^2),\quad j=1,2,\ldots,M. \tag{A11b}$$

The ion charged density is

$$\rho=e\sum_l(-1)^{\upsilon_l}Z_l\tilde{n}_l. \tag{A12}$$

Use Eqs. (A11) and (A6), under the condition of long-wavelength approximation, only when $\omega^2=\omega_{\mathrm{p}}^2+\beta^2k^2$, $\rho\neq0$; otherwise $\rho=0$. That is to say, $\omega^2=\omega_{\mathrm{p}}^2+\beta^2k^2$ represents ion charged density wave, and can be coupled with MTs by dipole–charge interactions as shown in Fig. 2. Other $M-1$ kinds of waves could not couple with MTs under the condition of long-wavelength approximation.

Finally, diagonalize matrix Ω

$$P(k)^{-1}\Omega(\omega(k),k)P(k)=\mathrm{diag}\{\omega_1\cdots,\omega_M\}. \tag{A13}$$

Set $P(k)=P(0)+O(k^2)$ and define another variable $\rho=(\rho_1,\rho_2,\ldots,\rho_M)^{\mathrm{T}}$, which is determined by

$$n=P(0)\rho+O(k^2). \tag{A14}$$

CPB Online In-Press

The transformation between n and ρ is

$$\begin{cases} \tilde{n}_1 = \dfrac{1}{\omega_{\rm p}^2}\sum\limits_{l=1}^{M}(-1)^{\upsilon_l}\dfrac{\omega_l^2}{Z_l}\rho_l \\ \tilde{n}_j = \dfrac{\omega_j^2}{\omega_{\rm p}^2}\left[\dfrac{(-1)^{\upsilon_j}}{Z_j}\rho_1 - \dfrac{1}{Z_j}\rho_j\right] \\ \qquad j = 2,3,\ldots,M. \end{cases} \tag{A15}$$

Then

$$\rho_1 = \sum_l (-1)^{\upsilon_l} Z_l \tilde{n}_l. \tag{A16}$$

Compare Eqs. (A16) and (A11), then

$$\rho = e\rho_1. \tag{A17}$$

So $e\rho_1$ could also be used to represent net charge density of ions, and equations (A15) and (A17) will be used in Appendix B.

Appendix B: Second quantization of environment Hamiltonian $H_{\rm e}$ and interaction Hamiltonian $H_{\rm in}$

In the coordinate representation, the Hamiltonian $H_{\rm e}$ of cellular environment can be shown as follows:

$$\hat{H}_{\rm e} = -\sum_{k,j}\frac{\left[\boldsymbol{p}_{k,j} + q_k\boldsymbol{A}(\boldsymbol{r}_{k,j},t)\right]^2}{2m_k} + q_k\phi(\boldsymbol{r}_{k,j},t), \tag{B1}$$

where $\boldsymbol{r}_{k,i}$ represents the position of the k-th kind of ions that have been numbered i, ϕ, $\boldsymbol{A}$ are scalar potential and vector potential, respectively, and $\boldsymbol{p}_{k,j} = \dfrac{\hbar}{\mathrm{i}}\nabla_{k,j}$ is the canonical momentum. The first term represents the kinetic energy of the ions, and the second term represents the field energy.

The potentials ϕ, $\boldsymbol{A}$ are not unique. For two different potentials $(\phi,\boldsymbol{A}),(\phi',\boldsymbol{A}')$, if they satisfy

$$\phi' = \phi - \frac{\partial\xi}{\partial t},\quad \boldsymbol{A}' = \boldsymbol{A} + \nabla\xi \quad \forall\xi, \tag{B2}$$

the two potentials will have the same field $\boldsymbol{E}$, $\boldsymbol{B}$ as follows:

$$\boldsymbol{E} = -\nabla\phi - \frac{\partial\boldsymbol{A}}{\partial t}, \boldsymbol{B} = \nabla\times\boldsymbol{A}. \tag{B3}$$

We use an approach similar to the David Bohm's electron gas model and define the Hamiltonian Eq. (B1) in another manner;[33] the second term is derived from the interactions between ions and the energy stored in the field. Therefore, equation (B1) can be written in an equivalent way as follows:

$$\hat{H}_{\rm e} = \sum_{k,j}\frac{\left[\boldsymbol{p}_{k,j} + q_k\boldsymbol{A}(\boldsymbol{r}_{k,j},t)\right]^2}{2m_k} + \int\frac{1}{2}\varepsilon|\boldsymbol{E}(\boldsymbol{r})|^2 + \frac{|\boldsymbol{B}(\boldsymbol{r})|^2}{2\mu}\mathrm{d}^3\boldsymbol{r}. \tag{B4}$$

First, set $\xi = \int\phi\,\mathrm{d}t$ so that $\phi' = 0$, then $\boldsymbol{E} = -\partial\boldsymbol{A}/\partial t$, $\boldsymbol{B} = \nabla\times\boldsymbol{A}$. Expand $\boldsymbol{A}$ in Fourier series $\exp(\mathrm{i}\boldsymbol{k}\cdot\boldsymbol{r})$

$$\begin{cases} \boldsymbol{A}_\parallel = \sum\limits_{\boldsymbol{k}} q(\boldsymbol{k})\boldsymbol{e}_{\boldsymbol{k}}\exp(\mathrm{i}\boldsymbol{k}\cdot\boldsymbol{r}) \\ \boldsymbol{A}_\perp = \sum\limits_{\boldsymbol{k},\mu=1,2} Q_\mu(\boldsymbol{k})\boldsymbol{e}_{\boldsymbol{k}\mu}\exp(\mathrm{i}\boldsymbol{k}\cdot\boldsymbol{r}), \end{cases} \tag{B5}$$

where $\boldsymbol{e}_{\boldsymbol{k}} = \boldsymbol{k}/k$ is an unit vector parallel to the direction of the wave propagation, $\boldsymbol{e}_{\boldsymbol{k}\mu}$ $(\mu = 1,2)$ is another two-unit vector which is perpendicular to $\boldsymbol{e}_{\boldsymbol{k}}$, and $\boldsymbol{e}_{\boldsymbol{k}1}\perp\boldsymbol{e}_{\boldsymbol{k}2}$. So $\boldsymbol{A}_\parallel$ and $\boldsymbol{A}_\perp$ represent longitudinal wave and transverse wave, respectively. Their electric field and magnetic field are

$$\begin{cases} \boldsymbol{E}_\parallel = \sum\limits_{\boldsymbol{k}} p(-\boldsymbol{k})\boldsymbol{e}_{\boldsymbol{k}}\exp(\mathrm{i}\boldsymbol{k}\cdot\boldsymbol{r}), \\ \boldsymbol{B}_\parallel = \sum\limits_{\boldsymbol{k}} q(\boldsymbol{k})(\mathrm{i}\boldsymbol{k}\times\boldsymbol{e}_{\boldsymbol{k}})\exp(\mathrm{i}\boldsymbol{k}\cdot\boldsymbol{r}) = 0, \end{cases} \tag{B6a}$$

$$\begin{cases} \boldsymbol{E}_\perp = \sum\limits_{\boldsymbol{k},\mu=1,2} P_\mu(-\boldsymbol{k})\boldsymbol{e}_{\boldsymbol{k}\mu}\exp(\mathrm{i}\boldsymbol{k}\cdot\boldsymbol{r}), \\ \boldsymbol{B}_\perp = \sum\limits_{\boldsymbol{k},\mu=1,2} Q_\mu(\boldsymbol{k})(\mathrm{i}\boldsymbol{k}\times\boldsymbol{e}_{\boldsymbol{k}\mu})\exp(\mathrm{i}\boldsymbol{k}\cdot\boldsymbol{r}), \end{cases} \tag{B6b}$$

where $p(-\boldsymbol{k}) = \dot{q}(\boldsymbol{k}), P_\mu(-\boldsymbol{k}) = \dot{Q}_\mu(\boldsymbol{k})$. $\boldsymbol{A}$ and $\boldsymbol{E}$ are real and can be ensured as follows:

$$\begin{cases} q(\boldsymbol{k}) = -q^*(-\boldsymbol{k}), \\ p(\boldsymbol{k}) = -p^*(-\boldsymbol{k}), \\ Q_\mu(\boldsymbol{k}) = Q_\mu^*(-\boldsymbol{k}), \\ P_\mu(\boldsymbol{k}) = P_\mu^*(-\boldsymbol{k}). \end{cases} \tag{B7}$$

Use Eqs. (B5) and (B6) as well as the commutative relation $[\hat{p},\boldsymbol{A}] = -\mathrm{i}\hbar\nabla\cdot\boldsymbol{A}$, the Hamiltonian equation (B4) will become

$$\hat{H}_{\rm e} = \hat{T} + \hat{H}_0 + \hat{H}_L + \hat{H}_T, \tag{B8}$$

where

$$\begin{cases} \hat{T} = \sum\limits_{l,j}\dfrac{p_{l,j}^2}{2m_l}, \\ \hat{H}_0 = -\sum\limits_{l,j}\dfrac{q_l}{2m_l}\left(2\boldsymbol{p}_{l,j} + \mathrm{i}\hbar\nabla_{l,j}\right)\cdot\boldsymbol{A}, \\ \hat{H}_{\rm L} = \sum\limits_{k,j}\dfrac{q_k^2\boldsymbol{A}_\parallel^2(\boldsymbol{r}_{k,j},t)}{2m_k} + \int\dfrac{\varepsilon|\boldsymbol{E}_\parallel(\boldsymbol{r})|^2}{2}\mathrm{d}^3\boldsymbol{r}, \\ \hat{H}_{\rm T} = \sum\limits_{k,j}\dfrac{q_k^2\boldsymbol{A}_\perp^2(\boldsymbol{r}_{k,j},t)}{2m_k} + \int\dfrac{\varepsilon|\boldsymbol{E}_\perp(\boldsymbol{r})|^2}{2} + \dfrac{|\boldsymbol{B}_\perp(\boldsymbol{r})|^2}{2\mu}\mathrm{d}^3\boldsymbol{r}. \end{cases} \tag{B9}$$

Now, use Eq. (B5), then we have

$$\sum_{k,j}\frac{q_k^2\boldsymbol{A}_\parallel^2(\boldsymbol{r}_{k,j},t)}{2m_k} = \sum_{l,j,\boldsymbol{k},\boldsymbol{g}}\frac{q_l^2}{2m_l}\boldsymbol{e}_{\boldsymbol{k}}\cdot\boldsymbol{e}_{\boldsymbol{g}}q(\boldsymbol{k})q(\boldsymbol{g})\exp[i(\boldsymbol{k}+\boldsymbol{g})\cdot\boldsymbol{r}_{l,j}] = \sum_{l,j,\boldsymbol{k}=-\boldsymbol{g}}\frac{q_l^2}{2m_l}\boldsymbol{e}_{\boldsymbol{k}}\cdot\boldsymbol{e}_{\boldsymbol{g}}q(\boldsymbol{k})q(\boldsymbol{g})\exp[\mathrm{i}(\boldsymbol{k}+\boldsymbol{g})\cdot\boldsymbol{r}_{l,j}]$$

CPB Online In-Press

$$+\sum_{l,j,\boldsymbol{k}\neq-\boldsymbol{g}}\frac{q_l^2}{2m_l}\boldsymbol{e}_{\boldsymbol{k}}\cdot\boldsymbol{e}_{\boldsymbol{g}}q(\boldsymbol{k})q(\boldsymbol{g})\exp[\mathrm{i}(\boldsymbol{k}+\boldsymbol{g})\cdot\boldsymbol{r}_{l,j}]$$
$$=-\sum_{l,\boldsymbol{k}}\frac{q_l^2 n_l}{2m_l}q(\boldsymbol{k})q(-\boldsymbol{k})+\sum_{l,j,\boldsymbol{k}\neq-\boldsymbol{g}}\frac{q_l^2}{2m_l}\boldsymbol{e}_{\boldsymbol{k}}\cdot\boldsymbol{e}_{\boldsymbol{g}}q(\boldsymbol{k})q(\boldsymbol{g})\exp[\mathrm{i}(\boldsymbol{k}+\boldsymbol{g})\cdot\boldsymbol{r}_{l,j}], \tag{B10}$$

where n_l is the number of l-th kind of ions in a unit volume. The random phase approximation (RPA) makes the second term in Eq. (B10) $\sum_{l,j,\boldsymbol{k}\neq-\boldsymbol{g}}$ considerably smaller than the first term $\sum_{l,j,\boldsymbol{k}=-\boldsymbol{g}}$; therefore

$$\sum_{k,j}\frac{q_k^2\boldsymbol{A}_{\parallel}^2(\boldsymbol{r}_{k,j},t)}{2m_k}=-\frac{\varepsilon}{2}\sum_{\boldsymbol{k}}\omega_{\mathrm{p}}^2q(\boldsymbol{k})q(-\boldsymbol{k}). \tag{B11}$$

Similarly,

$$\sum_{k,j}\frac{q_k^2\boldsymbol{A}_{\perp}^2(\boldsymbol{r}_{k,j},t)}{2m_k}=\frac{\varepsilon}{2}\sum_{\boldsymbol{k},\mu=1,2}\omega_{\mathrm{p}}^2Q_{\mu}(-\boldsymbol{k})Q_{\mu}(\boldsymbol{k}). \tag{B12}$$

Use Eqs. (B6a) and (B6b), then we obtain

$$\int\frac{\varepsilon|\boldsymbol{E}_{\parallel}(\boldsymbol{r})|^2}{2}\mathrm{d}^3\boldsymbol{r}=-\frac{\varepsilon}{2}\sum_{\boldsymbol{k}}p(\boldsymbol{k})p(-\boldsymbol{k}), \tag{B13a}$$
$$\int\frac{\varepsilon|\boldsymbol{E}_{\perp}(\boldsymbol{r})|^2}{2}+\frac{|\boldsymbol{B}_{\perp}(\boldsymbol{r})|^2}{2\mu}\mathrm{d}^3\boldsymbol{r}=\frac{\varepsilon}{2}\sum_{\boldsymbol{k},\mu=1,2}\left[P_{\mu}(-\boldsymbol{k})P_{\mu}(\boldsymbol{k})+c^2k^2Q_{\mu}(-\boldsymbol{k})Q_{\mu}(\boldsymbol{k})\right]. \tag{B13b}$$

$\hat{T}=\sum_{l,j}\frac{\boldsymbol{p}_{l,j}^2}{2m_l}$ means the kinetic energy, and it can be divide it into two parts

$$\sum_{l,j}\frac{\boldsymbol{p}_{l,j}^2}{2m_l}=\sum_l\int\left[\frac{n_lm_l|\boldsymbol{u}_l|^2}{2}+\frac{m_l\beta_l^2|\tilde{n}_l|^2}{2\langle n_l\rangle}\right]\mathrm{d}\boldsymbol{r}. \tag{B14}$$

The first term is the macroscopical translational energy, and the second term means the thermodynamic energy.

The second term in Eq. (B14) can be changed into

$$\sum_l\int\frac{m_l\beta_l^2|\tilde{n}_l|^2}{2\langle n_l\rangle}\mathrm{d}\boldsymbol{r}=\sum_{l,\boldsymbol{k}}\frac{m_l\beta_l^2|\tilde{n}_l(\boldsymbol{k})|^2}{2\langle n_l\rangle}. \tag{B15}$$

Now, use Eq. (A15) and ignore the cross term $\rho_i\rho_j$ $(i\neq j)$, then

$$\sum_{l,\boldsymbol{k}}\frac{m_l\beta_l^2|\tilde{n}_l|^2}{2\langle n_l\rangle}=\frac{e^2}{\varepsilon}\left(\frac{\beta^2|\rho_1|^2}{2\omega_{\mathrm{p}}^2}+\sum_{\boldsymbol{k},l=2}\frac{\beta_l^2\omega_l^4|\rho_l|^2}{Z_l^2\omega_{\mathrm{p}}^4}\right). \tag{B16}$$

As discussed in Appendix A, $e\rho_1$ represents net charge density of ions, so use Gauss's theorem in $\boldsymbol{k}$-space

$$\rho(\boldsymbol{k})=e\rho_1=\mathrm{i}\varepsilon\boldsymbol{k}\cdot\boldsymbol{E}=\mathrm{i}\varepsilon kp(-\boldsymbol{k}). \tag{B17}$$

Use Eqs. (B8)–(B17), then the total Hamiltonian is expressed by

$$\hat{H}_{\mathrm{e}}=\left[\sum_l\int\frac{n_lm_l|\boldsymbol{u}_l|^2}{2}\mathrm{d}\boldsymbol{r}+\sum_{\boldsymbol{k},l=2}\frac{\beta_l^2\omega_l^4|\rho_l|^2}{Z_l^2\omega_{\mathrm{p}}^4}\right]$$
$$-\sum_{l,j}\frac{q_l}{2m_l}\left(2\boldsymbol{p}_{l,j}+\mathrm{i}\hbar\nabla_{l,j}\right)\cdot\boldsymbol{A}$$
$$+\frac{\varepsilon}{2}\sum_{\boldsymbol{k},\mu=1,2}\left[P_{\mu}(-\boldsymbol{k})P_{\mu}(\boldsymbol{k})+\Omega_1^2(k)Q_{\mu}(-\boldsymbol{k})Q_{\mu}(\boldsymbol{k})\right]$$
$$-\frac{1}{2}\varepsilon\sum_{\boldsymbol{k}}\left[\omega_{\mathrm{p}}^2q(\boldsymbol{k})q(-\boldsymbol{k})+\frac{\Omega_2^2(k)}{\omega_{\mathrm{p}}^2}p(\boldsymbol{k})p(-\boldsymbol{k})\right], \tag{B18}$$

where the first term means ion sound wave, the second term means interaction between ions and fields and it is neglected for the reason that each ion has a random phase (random phase approximation or RPA), $\Omega_1^2(k)=\omega_{\mathrm{p}}^2+c^2k^2$ is the dispersion relation of electromagnetic wave in plasma, and $\Omega_2^2(k)=\omega_{\mathrm{p}}^2+\beta^2k^2$ is the dispersion relation of charged density wave or plasma oscillation.

At last, using second quantization method, define $\hat{A}_{\mu}^{\dagger}(\boldsymbol{k}),\hat{A}_{\mu}(\boldsymbol{k})$ as the creation operator and annihilation operator of electromagnetic wave, respectively, and $\hat{a}^{\dagger}(\boldsymbol{k})$ and $\hat{a}(\boldsymbol{k})$ as the creation operator and annihilation operator of the plasma oscillations, respectively, and we can obtain

$$\begin{cases}Q_{\mu}(\boldsymbol{k})=\sqrt{\dfrac{\hbar}{2\varepsilon\Omega(\boldsymbol{k})}}\left[\hat{A}_{\mu}(\boldsymbol{k})-\hat{A}_{\mu}^{\dagger}(-\boldsymbol{k})\right],\\ P_{\mu}(\boldsymbol{k})=-\mathrm{i}\sqrt{\dfrac{\hbar\Omega(\boldsymbol{k})}{2\varepsilon}}\left[\hat{A}_{\mu}(\boldsymbol{k})-\hat{A}_{\mu}^{\dagger}(-\boldsymbol{k})\right],\end{cases} \tag{B19a}$$

$$\begin{cases}q(\boldsymbol{k})=\sqrt{\dfrac{\hbar}{2\varepsilon\omega(\boldsymbol{k})}}\left[\hat{a}(\boldsymbol{k})-\hat{a}^{\dagger}(-\boldsymbol{k})\right],\\ p(\boldsymbol{k})=\mathrm{i}\sqrt{\dfrac{\hbar\omega(\boldsymbol{k})}{2\varepsilon}}\left[\hat{a}^{\dagger}(\boldsymbol{k})+\hat{a}(-\boldsymbol{k})\right].\end{cases} \tag{B19b}$$

And $\hat{A}_{\mu}^{\dagger}(\boldsymbol{k}),\hat{A}_{\mu}(\boldsymbol{k}),\hat{a}^{\dagger}(\boldsymbol{k}),\hat{a}(\boldsymbol{k})$ satisfy the commutation

CPB Online In-Press

relation

$$\begin{cases} \left[\hat{A}^{\dagger}_{\mu}(\boldsymbol{k}_1),\hat{A}^{\dagger}_{\nu}(\boldsymbol{k}_2)\right] = \left[\hat{A}_{\mu}(\boldsymbol{k}_1),\hat{A}_{\nu}(\boldsymbol{k}_2)\right] = 0, \\ \left[\hat{A}_{\mu}(\boldsymbol{k}_1),\hat{A}^{\dagger}_{\nu}(\boldsymbol{k}_2)\right] = \delta(\boldsymbol{k}_1-\boldsymbol{k}_2)\delta_{\mu\nu}, \\ \left[\hat{a}^{\dagger}(\boldsymbol{k}_1),\hat{a}^{\dagger}(\boldsymbol{k}_2)\right] = \left[\hat{a}(\boldsymbol{k}_1),\hat{a}(\boldsymbol{k}_2)\right] = 0, \\ \left[\hat{a}(\boldsymbol{k}_1),\hat{a}^{\dagger}(\boldsymbol{k}_2)\right] = \delta(\boldsymbol{k}_1-\boldsymbol{k}_2). \end{cases} \tag{B20}$$

Use Eqs. (B19) and (B20) and the random phase approximation, the Hamiltonian equation (B18) will become

$$\begin{aligned} \hat{H}_{\mathrm{e}} &= \sum_l \int \frac{n_l m_l |\boldsymbol{u}_l|^2}{2}\mathrm{d}\boldsymbol{r} + \sum_{\boldsymbol{k},l=2} \frac{\beta_l^2\omega_l^4|\rho_l|^2}{Z_l^2\omega_{\mathrm{p}}^4} \\ &+ \sum_{\boldsymbol{k},\mu=1,2} \hbar\Omega_1(\boldsymbol{k})\left[\hat{A}^{+}_{\mu}(\boldsymbol{k})\hat{A}^{+}_{\mu}(\boldsymbol{k}) + \frac{1}{2}\right] \\ &+ \sum_{\boldsymbol{k}} \hbar\omega(\boldsymbol{k})\left[\hat{a}^{\dagger}(\boldsymbol{k})\hat{a}(\boldsymbol{k}) + \frac{1}{2}\right], \end{aligned} \tag{B21}$$

where

$$\omega^2(\boldsymbol{k}) = \frac{\omega_{\mathrm{p}}^2}{1-\dfrac{\beta^2k^2}{\omega_{\mathrm{p}}^2}}. \tag{B22}$$

In long-wavelength limit, $\beta^2k^2/\omega_{\mathrm{p}}^2 \ll 1$, so

$$\omega^2(\boldsymbol{k}) = \omega_{\mathrm{p}}^2 + \beta^2k^2. \tag{B23}$$

This is the dispersion relation of ion charged density wave as shown in Appendix A.

In Eq. (B21), only the 3rd term could be coupled with MTs by dipole–charge interactions (as seen in Eq. (B17), $\rho(\boldsymbol{k})$ is only related to $p(\boldsymbol{k})$ instead of $P_{\mu}(\boldsymbol{k})$), so this model only considers the 3rd term which is named $\hat{H}_{\mathrm{pl}}$

$$\hat{H}_{\mathrm{pl}} = \sum_{\boldsymbol{k}} \hbar\omega(\boldsymbol{k})\left[\hat{a}^{\dagger}(\boldsymbol{k})\hat{a}(\boldsymbol{k}) + \frac{1}{2}\right], \tag{B24}$$

namely, the coupling between MTs and cellular environment via interactions between plasma oscillations and dipoles. The interaction Hamiltonian for a single dipole with the cellular environment is determined by Eq. (5). Thus, after Fourier transformation, equation (5) becomes

$$H' = \sum_{\boldsymbol{k}} \int \frac{\boldsymbol{p}\cdot\boldsymbol{r}}{4\pi\varepsilon|\boldsymbol{r}|^3}\rho(\boldsymbol{k})\exp(\mathrm{i}\boldsymbol{k}\cdot\boldsymbol{r})\mathrm{d}\boldsymbol{r}. \tag{B25}$$

According to Eqs. (B17) and (B19b), then

$$\rho(\boldsymbol{k}) = -k\sqrt{\frac{\hbar\varepsilon\omega(\boldsymbol{k})}{2}}\left[\hat{a}^{\dagger}(-\boldsymbol{k}) + \hat{a}(\boldsymbol{k})\right], \tag{B26}$$

the MT's dipole $\boldsymbol{p}$ can be written as follows:

$$\boldsymbol{p} = \sum_n \boldsymbol{p}_n \hat{c}_n^{\dagger}\hat{c}_n. \tag{B27}$$

Here, $\boldsymbol{p}_n = \langle n|\hat{\boldsymbol{p}}|n\rangle$ is the observed value of $\boldsymbol{p}$ in state $|n\rangle$. In Eq. (B27), the the cross term $\boldsymbol{p}_{m,n}\hat{c}_m^{\dagger}\hat{c}_n$ was neglected, use Eqs. (B25)–(B27), then the coupling Hamiltonian can be written as follows:

$$H' = \sum_{n,\boldsymbol{k}} H_{n,\boldsymbol{k}}, \tag{B28}$$

where

$$\begin{aligned} H_{n,\boldsymbol{k}} &= \lambda_{n,\boldsymbol{k}}\hat{c}_n^{\dagger}\hat{c}_n\left[\hat{a}^{\dagger}(-\boldsymbol{k}) + \hat{a}(\boldsymbol{k})\right], \\ \lambda_{n,\boldsymbol{k}} &= \frac{-k}{8\pi}\sqrt{\frac{\hbar\omega(\boldsymbol{k})}{2\varepsilon}}\int \frac{\boldsymbol{p}_n\cdot\boldsymbol{r}'}{|\boldsymbol{r}'|^3}\exp(\mathrm{i}\boldsymbol{k}\cdot\boldsymbol{r}')\mathrm{d}^3\boldsymbol{r}' \end{aligned} \tag{B29}$$

The $H_{n,\boldsymbol{k}}$ means the interaction between MTs and cellular fluid environment mentioned later, and it is then used to compute decoherence time, and $\lambda_{n,\boldsymbol{k}}$ is the coupling coefficient. The method for computing the coupling coefficient $\lambda_{n,\boldsymbol{k}}$ will be introduced in Appendix C.

Appendix C: Computation of coupling coefficient $\lambda_{n,\boldsymbol{k}}$

The coupling coefficient $\lambda_{n,\boldsymbol{k}}$ is expressed as follows:

$$\lambda_{n,\boldsymbol{k}} = \frac{\mathrm{i}k}{8\pi}\sqrt{\frac{\hbar\omega(\boldsymbol{k})}{2\varepsilon}}\int \frac{\boldsymbol{p}_n\cdot\boldsymbol{r}}{r^3}\exp(\mathrm{i}\boldsymbol{k}\cdot\boldsymbol{r})\mathrm{d}\boldsymbol{r}, \tag{C1}$$

where $\boldsymbol{p}_n$ is a constant vector; for a certain $\boldsymbol{k}$, the z axis is set to be parallel to $\boldsymbol{k}$. In the spherical coordinate frame, $\boldsymbol{k}\cdot\boldsymbol{r} = kr\cos\theta$, and the volume element $\mathrm{d}\boldsymbol{r} = r^2\sin\theta\,\mathrm{d}\theta\,\mathrm{d}\varphi$; thus, $\boldsymbol{p}_n$ can be expressed as follows:

$$\boldsymbol{p}_n = p_x\boldsymbol{e}_x + p_y\boldsymbol{e}_y + p_z\boldsymbol{e}_z. \tag{C2}$$

Thus,

$$\boldsymbol{p}_n\cdot\boldsymbol{r} = r\left[p_x\sin\theta\cos\varphi + p_y\sin\theta\sin\varphi + p_z\cos\theta\right]. \tag{C3}$$

When the variable φ is integrated in the interval $[0,2\pi]$, then

$$\begin{aligned} \lambda_{n,\boldsymbol{k}} &= \frac{-k}{8\pi}\sqrt{\frac{\hbar\omega(\boldsymbol{k})}{2\varepsilon}}\int p_z\cos\theta\exp(\mathrm{i}kr\cos\theta)\sin\theta\,\mathrm{d}r\mathrm{d}\theta\,\mathrm{d}\varphi \\ &= -\frac{kp_z}{4}\sqrt{\frac{\hbar\omega(\boldsymbol{k})}{2\varepsilon}}(A+\mathrm{i}B), \end{aligned} \tag{C4}$$

where

$$\begin{cases} A = \displaystyle\int_{r_{\min}}^{r_{\max}}\mathrm{d}r\int_0^{\pi}\cos\theta\cos(kr\cos\theta)\sin\theta\,\mathrm{d}\theta, \\ B = \displaystyle\int_{r_{\min}}^{r_{\max}}\mathrm{d}r\int_0^{\pi}\cos\theta\sin(kr\cos\theta)\sin\theta\,\mathrm{d}\theta. \end{cases} \tag{C5}$$

Compute Eq. (C5), then $A = 0$ and

$$B = \frac{2}{k}\left[\frac{\sin(kr_{\min})}{(kr_{\min})} - \frac{\sin(kr_{\max})}{(kr_{\max})}\right]. \tag{C6}$$

Here, $p_z = \boldsymbol{p}_n\cdot\boldsymbol{k}/k$; generally, in the actual situation, plasma oscillations will be excited only when the wavelength is larger than the Debye length λ_{D}. Therefore, only $k < 2\pi/\lambda_{\mathrm{D}}$ could be used to refer to the excited state. The integral in Eq. (C1) in the space $|\boldsymbol{r}| > \lambda_{\mathrm{D}}$ because a shielding layer charge appears on the surface of MTs with a thickness λ_{D}, as shown

CPB Online In Press

in Fig. 2. The shielding layer charge is stable and cannot excite plasma oscillations; therefore, in Eq. (C6), $r_{\min} = \lambda_{\rm D}$ and $r_{\max} = \infty$. Hence,

$$\lambda_{n,\boldsymbol{k}} = -\frac{\mathrm{i}\boldsymbol{p}_n \cdot \boldsymbol{k}}{2k}\sqrt{\frac{\hbar\omega(\boldsymbol{k})}{2\varepsilon}}\frac{\sin(k\lambda_{\rm D})}{(k\lambda_{\rm D})}. \tag{C7}$$

Define $b(\boldsymbol{k}) = -\mathrm{i}a(\boldsymbol{k})$ as new creation operator and annihilation operator, then the total Hamiltonian is

$$\begin{aligned}\hat{H} = &\sum_n \hbar\Omega_n \hat{c}_n^{\dagger}\hat{c}_n \\ &+\sum_n \hbar\omega(\boldsymbol{k})\left[\hat{b}^{\dagger}(\boldsymbol{k})\hat{b}(\boldsymbol{k}) + \frac{1}{2}\right] \\ &+\sum_{n,\boldsymbol{k}} \mu_{n,\boldsymbol{k}}\hat{c}_n^{\dagger}\hat{c}_n\left[\hat{b}^{\dagger}(\boldsymbol{k})\hat{b}(\boldsymbol{k})\right],\end{aligned}$$

where

$$\mu_{n,\boldsymbol{k}} = \mathrm{i}\lambda_{n,\boldsymbol{k}} = \frac{\boldsymbol{p}_n \cdot \boldsymbol{k}}{2k}\sqrt{\frac{\hbar\omega(\boldsymbol{k})}{2\varepsilon}}\frac{\sin(k\lambda_{\rm D})}{(k\lambda_{\rm D})},$$

and we have obtained Eqs. (7) and (8).

References

[1] Turin L 1996 *Chem. Senses* **21** 773
[2] Franco M I and Siddiqi O 2011 *Proc. Natl. Acad. Sci. USA* **108** 3797
[3] Ritz T, Adem S and Schulten K 2000 *Biophys. J.* **78** 707
[4] Hiscock H G, Worster S, Kattnig D R, Steers C, Jin Y, Manolopoulos D E, Mouritsen H and Hore P J 2016 *Proc. Natl. Acad. Sci. USA* **113** 201600341
[5] Gregory S E, Tessa R C, Elizabeth L R, Tae-Kyu A, Tomás M, Yuan-Chung C, Robert E B and Graham R F 2007 *Nature* **446** 782
[6] Romero E, Augulis R, Novoderezhkin V I, Ferretti M, Thieme J, Zigmantas D and Van Grondelle R 2014 *Nat. Phys.* **10** 676
[7] Levi F, Mostarda S, Rao F and Mintert F 2015 *Rep. Prog. Phys.* **78** 082001
[8] Novelli F, Nazir A, Richards G H, Roozbeh A, Wilk K E, Curmi P M and Davis J A 2015 *J. Phys. Chem. Lett.* **6** 4573
[9] Sarovar M, Ishizaki A, Fleming G and Whaley B 2010 *Nat. Phys.* **3** 462
[10] Marletto C, Coles D, Farrow T and Vedral V 2018 *J. Phys. Commun.* **2** 101001
[11] Mesquita M V, Vasconcellos Á R, Luzzi R and Mascarenhas S 2005 *Int. J. Quantum Chem.* **102** 1116
[12] Jackendoff R 1987 *Consciousness and the Computational Mind* (Cambridge: The MIT Press) pp. 275–280
[13] Tononi G, Boly M, Massimini M and Koch C 2016 *Nat. Rev. Neurosci.* **17** 450
[14] Crick F and Koch C 2003 *Nat. Neurosci.* **6** 119
[15] Edelman G M 2003 *Proc. Natl. Acad. Sci. USA* **100** 5520
[16] Jahn R G and Dunne B J 2007 *Found. Phys.* **3** 306
[17] Mershin A, Sanabria H, Miller J H, Nawarathna D, Skoulakis E M, Mavromatos N E, Kolomenskii A A, Schuessler H A, Luduena R F and Nanopoulos D V 2006 *The Emerging Physics of Consciousness* (Berlin: Springer) pp. 95–170
[18] Hameroff S and Penrose R 2014 *Phys. Life Rev.* **11** 39
[19] Hameroff S and Penrose R 2014 *Phys. Life Rev.* **11** 94
[20] Hameroff S R and Penrose R 2017 *Biophysics of Consciousness: A Foundational Approach* (Singapore: World Scientific) pp. 517–599
[21] Craddock T J A and Tuszynski J A 2010 *J. Biol. Phys.* **36** 53
[22] Craddock T J, Priel A and Tuszynski J A 2014 *J. Integr. Neurosci.* **13** 293
[23] Fisher M 2015 *Ann. Phys.* **61** 593
[24] Hameroff S R 2007 *Cogn. Sci.* **31** 1035
[25] Mavromatos N E, Mershin A and Nanopoulos D V 2002 *Int. J. Mod. Phys. B* **16** 3623
[26] Mavromatos N 1999 *Bioelectrochemistry Bioenergetics* **48** 273
[27] Tegmark M 2000 *Phys. Rev. E* **61** 4194
[28] Hagan S, Hameroff S R and Tuszyński J A 2002 *Phys. Rev. E* **65** 061901
[29] Nelson P 2007 *Biological Physics* (New York: WH Freeman) p. 416
[30] Priel A, Tuszynski J A and Woolf N J 2005 *Eur. Biophys. J. Biophys. Lett.* **35** 40
[31] Privman V and Tolkunov D 2005 *Quantum Information and Computation III* (Bellingham: The International Society for Optics and Photonics), pp. 187–195
[32] Tolkunov D, Privman V and Aravind P K 2005 *Phy. Rev. A* **71** 060308
[33] Craddock T J, Friesen D, Mane J, Hameroff S and Tuszynski J A 2014 *J. R. Soc. Interface* **11** 20140677
[34] Chen Y, Okur H I, Gomopoulos N, Macias-Romero C, Cremer P S, Petersen P B, Tocci G, Wilkins D M, Liang C and Ceriotti M 2016 *Sci. Adv.* **2** e1501891
[35] Fröhlich H 1968 *Int. J. Quantum Chem.* **2** 641
[36] Wu T M and Austin S J 1981 *J. Biol. Phys.* **9** 97
[37] Bohm D and Pines D 1953 *Phy. Rev.* **92** 609
[38] Yin C C and Biophysics D O 2018 *Chin. Phys. B* **27** 058703
[39] Zheng C J, Jia T Q, Zhao H, Xia Y J, Zhang S A and Sun Z R 2018 *Chin. Phys. B* **27** 057802
[40] Wade C G, Šibalić N, de Melo N R, Kondo J M, Adams C S and Weatherill K J 2017 *Nat. Photon.* **11** 40
[41] Trocha P, Karpov M, Ganin D, Pfeiffer M H, Kordts A, Wolf S, Krockenberger J, Marin-Palomo P, Weimann C and Randel S 2018 *Science* **359** 887

CPB Online In Press